**NASA TECHNICAL MEMORANDUM**

NASA TM X-52698

NASA TM X-52698



# PERFORMANCE OF A HERMETIC INDUCTION MOTOR-DRIVEN PUMP FOR BRAYTON CYCLE HEAT REJECTION LOOP

by Adolph C. Spagnuolo, Richard R. Secunde and James E. Vrancik
Lewis Research Center
Cleveland, Ohio
October 20, 1969

This information is being published in preliminary form in order to expedite its early release.

# PERFORMANCE OF A HERMETIC INDUCTION MOTOR-DRIVEN PUMP FOR BRAYTON CYCLE HEAT REJECTION LOOP

By Adolph C. Spagnuolo, Richard R. Secunde and James E. Vrancik

Lewis Research Center
Cleveland, Ohio

# PERFORMANCE OF A HERMETIC INDUCTION MOTOR-DRIVEN PUMP FOR BRAYTON CYCLE HEAT REJECTION LOOP

by Adolph C. Spagnuolo, Richard R. Secunde and James E. Vrancik

Lewis Research Center

E-5338

## SUMMARY

Two motor-driven pumps were tested in simulated Brayton cycle heat rejection loops using dimethyl polysiloxane (D.C.-200) coolant fluid. The pumps ran equally well on both 3-phase, 400 hertz, sine wave power and 400 hertz quasi-square wave input power from a static inverter. Pump pressure rise was at least 60 psi (41 $N/cm^2$) from zero flow to design flow of 3.7 gpm ($1.4X10^{-2}$ $m^3/min$).

Cavitation was heard at all flow rates when pump inlet pressure was reduced below 12 psia (8.3 $N/cm^2$). Pump performance however was not affected until flow separation occurred at inlet pressures less than 1 psia (0.7 $N/cm^2$). The pump continued to operate at a reduced pressure rise and flow rate and at no time did it stop pumping fluid completely.

## INTRODUCTION

The Brayton cycle engine is engineered to produce between 2 and 15 kilowatts of electrical power for future space applications (refs. 1 through 4). The powerplant consists of a heat source, a power conversion unit, a heat rejection system, and the engine controls. The heat rejection system is split to provide primary and secondary cooling in parallel loops sharing a common motor-driven pump. The coolant is dimethyl polysiloxane (D.C.-200) a silicone liquid.

Long life and reliability are prime requirements in all auxiliary space power systems. It is important then, that the heat rejection loop and the pump have zero external leakage. One way to be certain of zero leakage is to eliminate any need for seals in the pump by enclosing the motor and pump in a common housing, and completely welding all joints in the pump and rejection loop.

The purpose of this report is to present experimental performance characteristics of the hermetic motor-driven pump.

Two pumps were tested in simulated heat rejection loops shown in figure 1. Only one loop is shown in figure 1, the second loop is identical to that shown. The loops provide cooling for electronic equipment mounted on cold plates. The pumps and the coolant loops are part of the electrical subsystem of the Brayton cycle engine. The electrical subsystem is assembled as shown in figure 2 to evaluate its performance under simulated conditions. Pump performance is presented at various voltages with a sine wave input and a quasi-square wave input from a static inverter. The effect of cavitation on pump performance is also presented for one of the pumps at various voltages and at design flow rate of 3.7 gpm ($1.4X10^{-2}$ $m^3$/min).

Induction-motor-powered centrifugal pumps for space power generating systems have been reported in references 5 through 8. The pumps tested were designed and manufactured by Pesco for NASA Lewis Research Center under contract number NAS3-10935.

## PUMP DESCRIPTION

The motor-driven pump (fig. 3) is an integral hermetically sealed unit consisting of a centrifugal pump and a three-phase, 400 hertz, 0.36 horsepower (269 watts) wet motor mounted in a common housing. The designed pump net pressure rise is 60 psi (41 $N/cm^2$) minimum at 3.7 gal/min ($1.4X10^{-2}$ $m^3$/min) and at a motor (ac rms) line voltage of 39 to 47 volts. Nominal speed is 11,000 rpm ($6.9X10^4$ rad/min).

The motor rotor is supported on a shaft between two carbon sleeve bearings (fig. 4). The pump impeller is overhung on one end of the shaft. The ends of the sleeve bearing which is located between the impeller and motor rotor serves as a two way thrust bearing. A metallic filter of 2 micron ($2X10^{-6}$ m) nominal rating is located on the inlet side of the impeller. Fluid entering the unit passes in sequence through the filter, impeller, diffuser, and motor where it cools the rotor and stator windings by direct contact, and lubricates the bearing.

The cylindrical motor pump housing is clamped to the mounting bracket by means of two adjustable metal straps. By rotating the housing in the brackets, the orientation of the inlet and discharge lines can be readily changed.

The motor is equipped with iron-constantan thermocouples and a speed sensing device.

## TEST FACILITY

Each induction-motor-powered centrifugal pump assembly was tested in a simulated Brayton engine heat rejection loop shown in figure 1. Dimethyl polysiloxane (D.C.-200), a silicone liquid with a viscosity of two (2) centistokes at $77^{o}$ F ($298^{o}$ K), serves as the cooling fluid. The coldplates are used to remove waste heat from the electronic equipment in a vacuum environment. The accumulator allows for any differential thermal expansion and contraction of the pumped fluid (D.C.-200). And also provides a net positive suction head (NPSH) at the pump inlet. The pressure on the gas side of the accumulator is regulated to increase or decrease the pump NPSH (fig. 1).

The discharge flow of the pump is split to provide 0.58 gpm ($2.2X10^{-3}$ $m^3$/min) design flow through the coldplates and the balance travels through a bypass line which simulates the flow through other Brayton engine components. The two then unite and return to the suction side of the pump. Pressure readings are taken at the suction and discharge side of the pump. Flow meters are located in the main discharge line and in each of the two branch lines.

Electrical power is furnished to the pump by a static inverter. A dc supply provides the inverter input power at plus (+) and minus (-) 28 volts. This results in an effective input voltage of 56 volts. The inverter is a transformerless bridge type, and provides a 400 hertz, three-wire, three-phase output. The line-to-line output voltage is quasi-square wave in form and has a peak voltage approximately equal to the input voltage. Figure 5 shows both the idealized and actual line-to-line output voltage wave form. The pump motors are 400 hertz induction type and were designed specifically for operation with the inverter.

The three-phase sine wave power used to test the pumps was supplied by a 400 hertz motor-generator set. This sine wave power is used for preliminary ground testing only.

## INSTRUMENTATION

The instrumentation for the simulated heat rejection loop consists of turbine flow meters, cryogenic strain gage pressure transducers, copper-constantan and iron constantan thermocouples, and a Pirani-type vacuum gage.

Turbine flow meters are used to measure the discharge flow of the pump, flow to the coldplates, and flow through the bypass loop. The discharge and bypass flow meters have a flow range of 0.5 to 5.0 gal/min

($0.19X10^{-2}$ to $1.9X10^{-2}$ $m^3/min$). Full scale output for these meters is 1400 Hz. The coldplate flow meter has a full scale output of 1200 Hz at a flow rate of 2.5 gpm ($0.95X10^{-2}$ $m^2/min$). The output of the flow meters is connected to frequency-to-dc converters. The resultant dc voltage is sent through a calibration potentiometer to a dc meter for visual readout. The dc meters are controller type with a high and low limit setting. If the flow goes out of limits an alarm sounds to alert the operator. The accuracy at the dc meter is $\pm$ 4.0 percent of full scale.

The cryogenic strain gage pressures transducers are used to monitor the suction, discharge, and filter pressures of the pump. The inlet pressure to the coldplates and the accumulator pressure are also recorded. The transducers are designed to operate over a pressure range of 0 to 100 psi (0 to 69 $N/cm^2$) and provide a 20 millivolt full scale signal. The 20 mV signal is sent to an amplifier to produce a 10 volt dc full scale signal which in turn is read out on a 10 volt voltmeter.

The voltmeters are of the controller type with high and low limit settings. If the pressure goes out of limits an alarm sounds to alert the operator. The accuracy at the dc meters is $\pm$ 3.0 percent of full scale.

Copper-constantan thermocouples are used to measure the temperature of the dimethyl polysiloxane (D.C.-200) fluid in the coldplates. The thermocouples are spot-welded to a thin metal strap and the strap, in turn, spot-welded to the stainless steel tube with the thermocouples in between. The electrical signal from the thermocouples is fed to a $150^{o}$ F ($339^{o}$ K) reference oven. The output of the reference oven is connected to a multipoint strip chart recorder. Accuracy of the readings at the strip chart recorder is $\pm$ 0.3 percent.

A Pirani-type vacuum gauge was used to measure the pressure in the gas side of the accumulator. Pressure is indicated on two meter scales; one from 500 torr (67,000 $N/m^2$) to 0.1 torr (13 $N/m^2$); and the other from 100 micron (13 $N/m^2$) to 1 micron (0.13 $N/m^2$). The pressure was read directly from the gauge.

## RESULTS AND DISCUSSION

Two pumps were tested in identical simulated Brayton cycle heat rejection loops. Pressure rise, power input, and overall efficiency were plotted for various voltages at different flow rates. The effect of cavitation on the pump performance was also recorded as a function of pump-inlet net positive suction head (NPSH). The design of each pump is identical. The fabrication is also identical with one exception.

One of the nine holes in the diffuser deviated $12\frac{1}{2}^{o}$ (0.22 rad) from specifications (fig. 6). This deviation was accepted and the diffuser became part of pump-B.

Performance curves for pumps A and B are presented in figures 7 and 8. The pumps were run on three phase, 400 hertz, ac power at 33V, 38V, 43V, and 48V, line-to-line input voltages. The temperature of the fluid ranged from $29^{o}$ C ($302^{o}$ K) to $33^{o}$ C ($306^{o}$ K). As expected the input power increased as the voltage increased and therefore the pressure rise is greater at the higher voltages. The shape of the overall efficiency curve is approximately the same for both pumps. Pump A, however, is 1 to 2 percentage points higher throughout the flow range. The main differences is in the head or pressure rise. The pressure rise in pump A is even up to 2 gpm ($0.76X10^{-2}$ $m^3$/min) and reaches a peak at 3 gpm ($1.1X10^{-2}$ $m^3$/min) before dropping to a minimum value at maximum flow rate. The pressure rise in pump B is maximum at the lowest flow rate and gradually decreases until it reaches a minimum pressure rise at the maximum flow rate. The difference in pump performance is due to the machining difference in the diffuser. Both pumps, however, are within the design specifications of 60 psi minimum pressure rise (41 N/$cm^2$) at 3.7 gpm flow ($1.4X10^{-2}$ $m^3$/min) and 39 to 47 volts line to line. It is significant that the pumps also ran satisfactorily at 33 volts which is well below the design voltage range. The inlet pressure for pump A was maintained at 21 psia (14 N/$cm^2$); 14 psia (9.7 N/$cm^2$) for pump B. The pressure rise or total head is not effected by the inlet pressure as long as the inlet pressure remains above the critical NPSH.

The effect of cavitation on pump performance using sinusoidal power at line voltages of 35, 40, 45, and 50 volts (rms) and at design flow, 3.7 gpm ($1.4X10^{-2}$ $m^3$/min), is shown in figure 9. Pump B was chosen for this test. Fluid temperature ranged from $29^{o}$ C ($302^{o}$ K) to $33^{o}$ C ($306^{o}$ K). Cavitation as evidenced by sharp cracking sounds of very short duration could be heard coming from the pump housing at approximately 12 psia (8.3 N/$cm^2$) inlet pressure. The frequency of the noise is very low and disappears when the inlet pressure is increased above 12 psia (8.3 N/$cm^2$). The frequency of the noise begins to increase as the NPSH is reduced. The noise level and frequency were noted by the operator with the aid of a stethoscope.

The performance of the pump was unaffected until very low inlet pressures (1 psi ($6.9X10^3$ N/$m^2$) or less) caused flow separation. The design specifications only require the pump to deliver design head and flow at a minimum NPSH of 20 psi (14 N/$cm^2$). Even after flow separation and extensive vapor formation the pump continued to operate at a reduced pressure rise and flow rate and at no time did it stop pumping fluid completely. The continued performance at very low inlet pressures is due to the low vapor pressure of D.C.-200, 168 microns (0.00325 psia) at $90^{o}$ F (22.4 N/$m^2$ at $305^{o}$ K) and a gas-free system. A vacuum of 10 microns

(1.3 $N/m^2$) was established in the heat rejection loop before filling with D.C.-200. And a vacuum of 200 microns (27 $N/m^2$) was established above the D.C.-200 fill tank to ensure a gas-free system.

The pumps were next run with a static inverter. The input voltage was varied as seen in figures 10 and 11. The performance curves are very similar to the curves in figures 7 and 8. The input power and pressure rise is slightly lower then the sinusoidal results for the same input voltage. The overall efficiency of the pumps when supplied by the inverters is slightly higher at equal flow rates than when supplied by the 400 hertz sine wave except at the lower (33V) voltage. The difference at the higher voltages is within experimental error. The lower efficiency at the lowest (33V) voltage with the inverter supply is most probably caused by deterioration in the wave form output of the inverter. The inverters were designed to operate over an input voltage range of 50 to 60 volts dc. To obtain the 33 volts ac output, the input voltage was 42.5 dc which is well below the minimum design point.

The effect of cavitation on pump performance using the static inverter power at various voltages is shown in figure 12. The results are similar to those obtained with sine wave power shown in figure 9. The cracking sounds were heard at approximately 12 psia (8.3 $N/cm^2$) and increased as the inlet pressure was lowered. Flow separation and extensive vapor formation occurred at a slightly higher NPSH with the inverter power. But as with sine wave power the pump continued to operate at a reduced pressure rise and flow rate and at no time did it stop pumping fluid completely.

Motor shaft speed in rpm is shown in figure 13 for different flow rates for pump B with inverter power. As expected the speed increases with increased voltage and becomes less dependent on fluid flow or load.

## SUMMARY OF RESULTS

Two pumps were tested in a simulated Brayton cycle heat rejection loop using dimethyl polysiloxane (D.C.-200) coolant fluid. The pumps ran equally well on both 3-phase, 400 hertz, sine wave power and quasi-square wave input power from a static inverter, meeting specifications in both cases. Both pumps met the design pressure rise of 60 psi (41 $N/cm^2$) minimum at design flow of 3.7 gpm ($1.4X10^{-2}$ $m^2/min$) when within the design motor line voltage range of 39 to 47 volts (rms).

Cavitation, evidenced by sharp cracking sounds, occurred at pump inlet pressure of approximately 12 psia (8.3 $N/cm^2$). The noise frequency increased as the inlet pressure was decreased. Pump performance, however, was not affected until flow separation occurred at inlet pressures less

than 1 psia (0.7 $N/cm^2$). After flow separation and extensive vapor formation, the pump continued to operate at a reduced pressure rise and flow rate and at no time did it stop pumping fluid completely.

## REFERENCES


1. Stewart, W. L.; et al: Brayton Cycle Systems. Selected Technology for the Electric Power Industry. NASA SP-5057, 1968, pp. 91-137.

2. Brown, William J.: Brayton-B Power System - A Progress Report. NASA TM X-52635. 1969.

3. Glassman, Arthur J.: Computer Program for Thermodynamic Performance of Brayton-Cycle Space-Power Systems. NASA TM X-1339, 1967.

4. Thomas, Ronald L.: Turboalternator Speed Control with Valves in Two-Spool Solar-Brayton System. NASA TN D-3783, 1967.

5. Gorland, Sol H.; Lottig, Roy A.; and Hecker, Thomas P.: Performance and Evaluation of a Liquid-Metal Pump for Mercury Service. NASA TM X-1766, 1969.

6. Chalplin, E. S.; Colker, C. P.; and Foss, C. L.: Design and Development of Pumps for High Temperature NaK Service. AIAA Specialists Conference on Rankine Space Power Systems. Vol. 1. AEC Rep. CONF-651026, vol. 1, 1965, pp. 186-200.

7. Chalpin, E. S.; Pope, J. R.; and Foss, C. L.: Development of a SNAP-8 Pump for Mercury Service. AIAA Specialists Conference on Rankine Space Power Systems. Vol. 1. AEC Rep. CONF-651026, vol. 1, 1965, pp. 171-185.

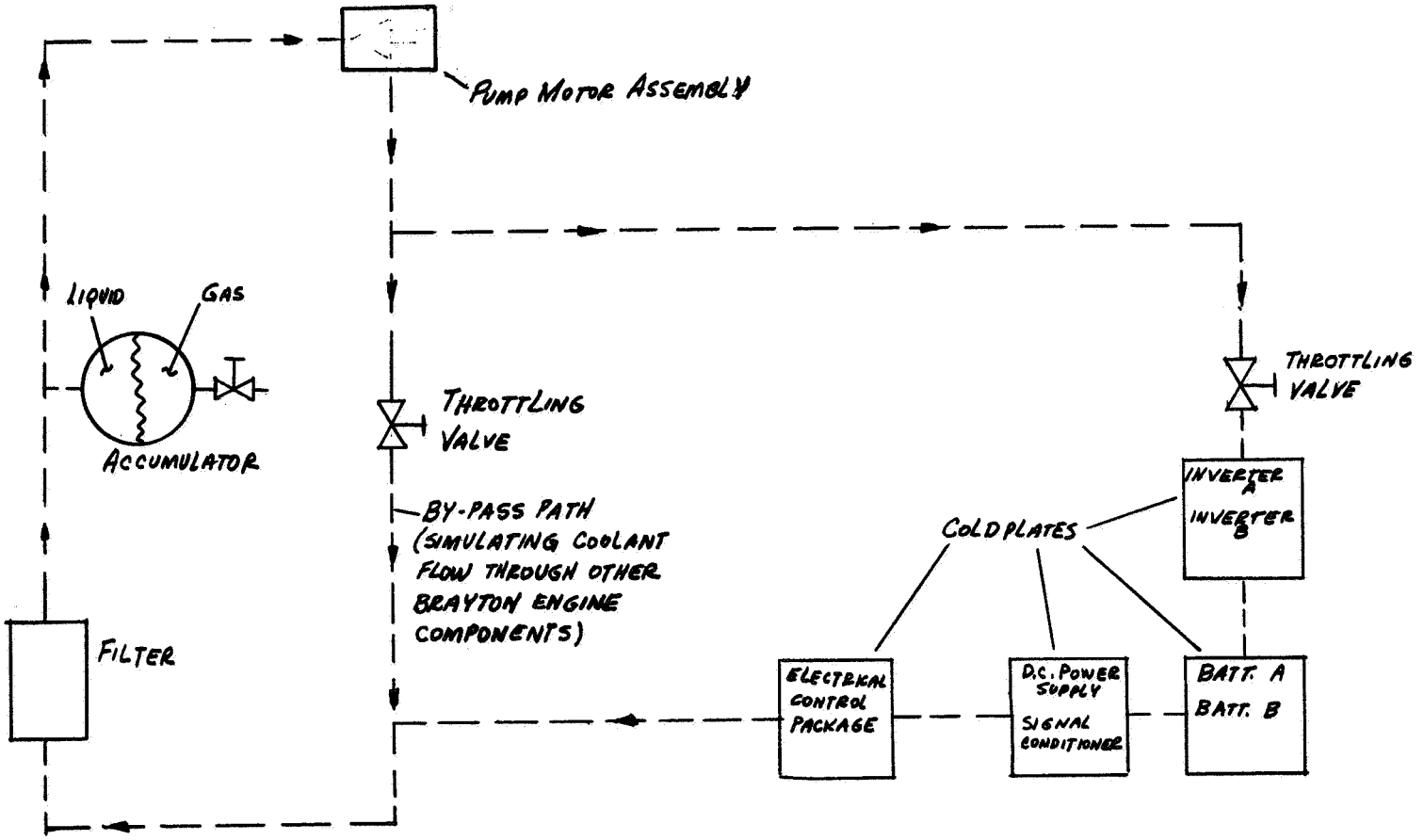


NOTE: THE SECOND COOLANT LOOP IS NOT SHOWN

FIG. 1 - SCHEMATIC of SIMULATED HEAT REJECTION LOOP for BRAYTON CYCLE SYSTEM

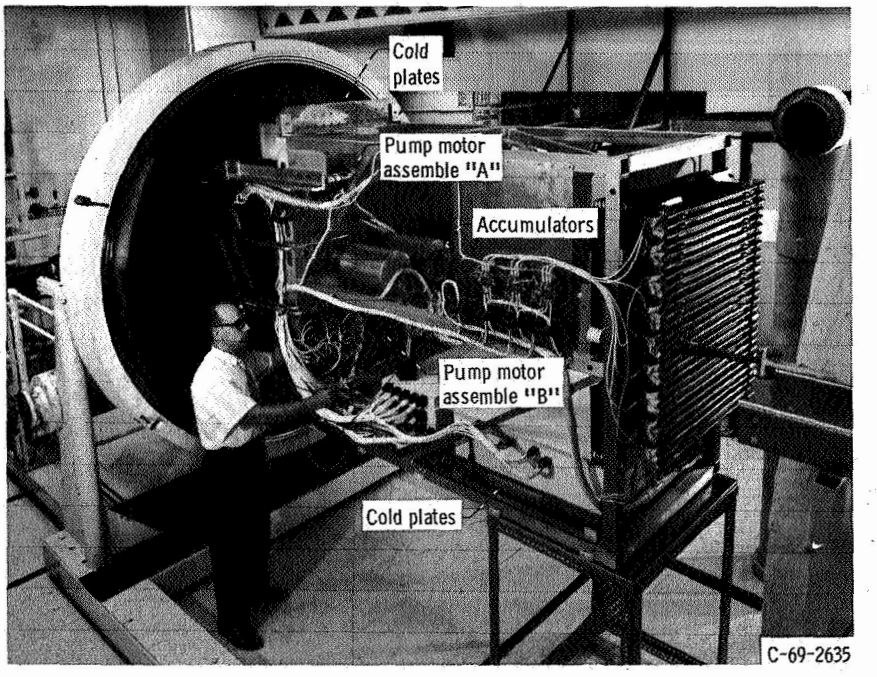


Fig. 2. - Brayton cycle electrical subsystem with simulated heat rejection loop.

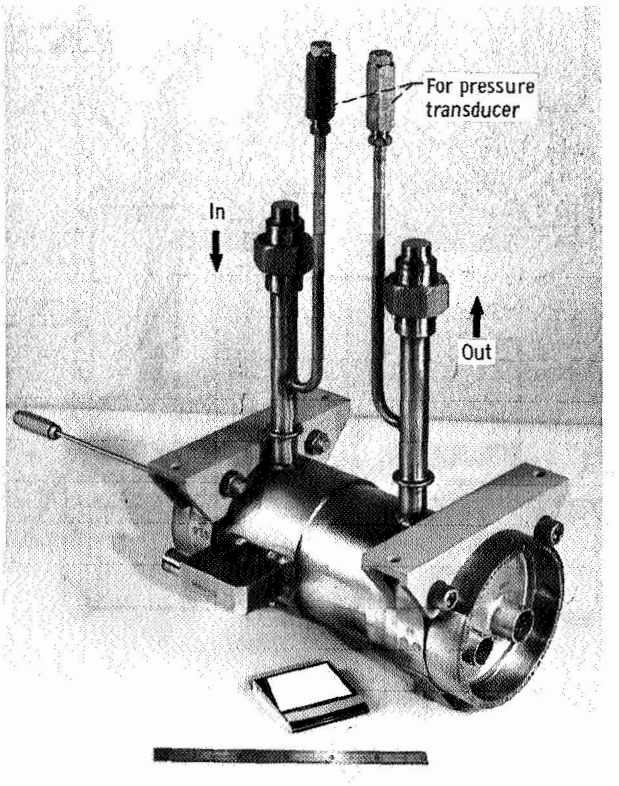


Fig. 3. - Pump motor assembly for Brayton cycle heat rejection loop.

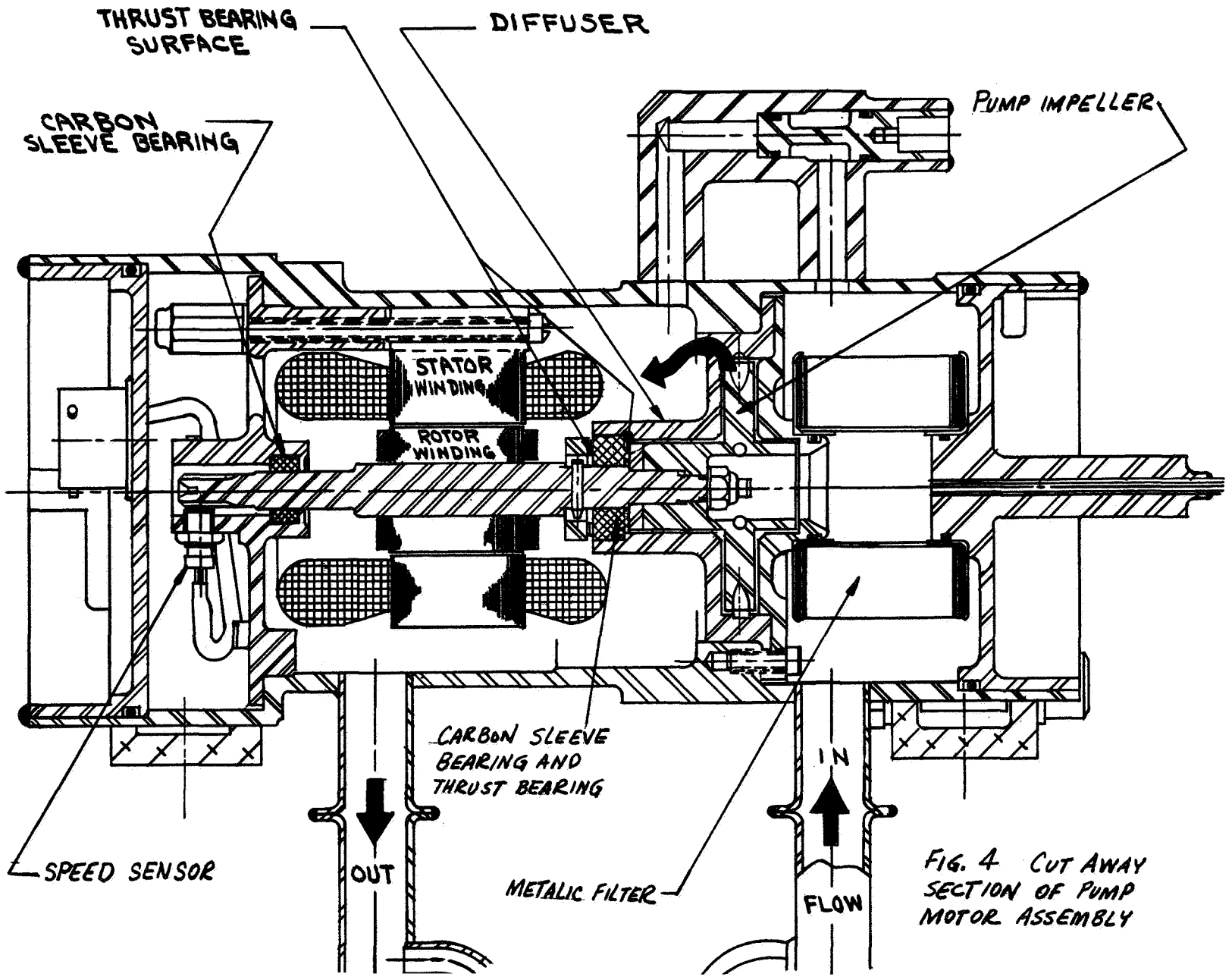


FIG. 4 CUT AWAY SECTION OF PUMP MOTOR ASSEMBLY

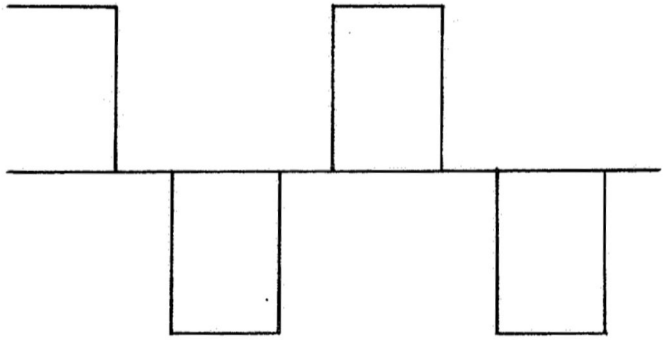

a. IDEAL

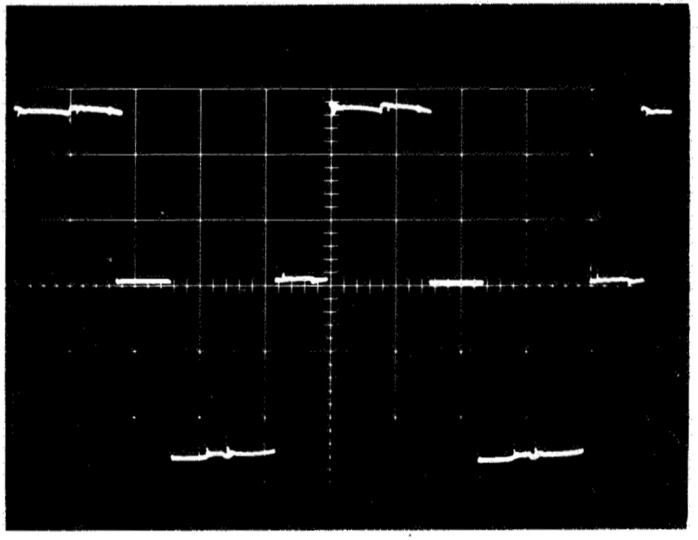

b. ACTUAL

FIGURE 5 INVERTER LINE-TO-LINE OUTPUT VOLTAGE WAVEFORM

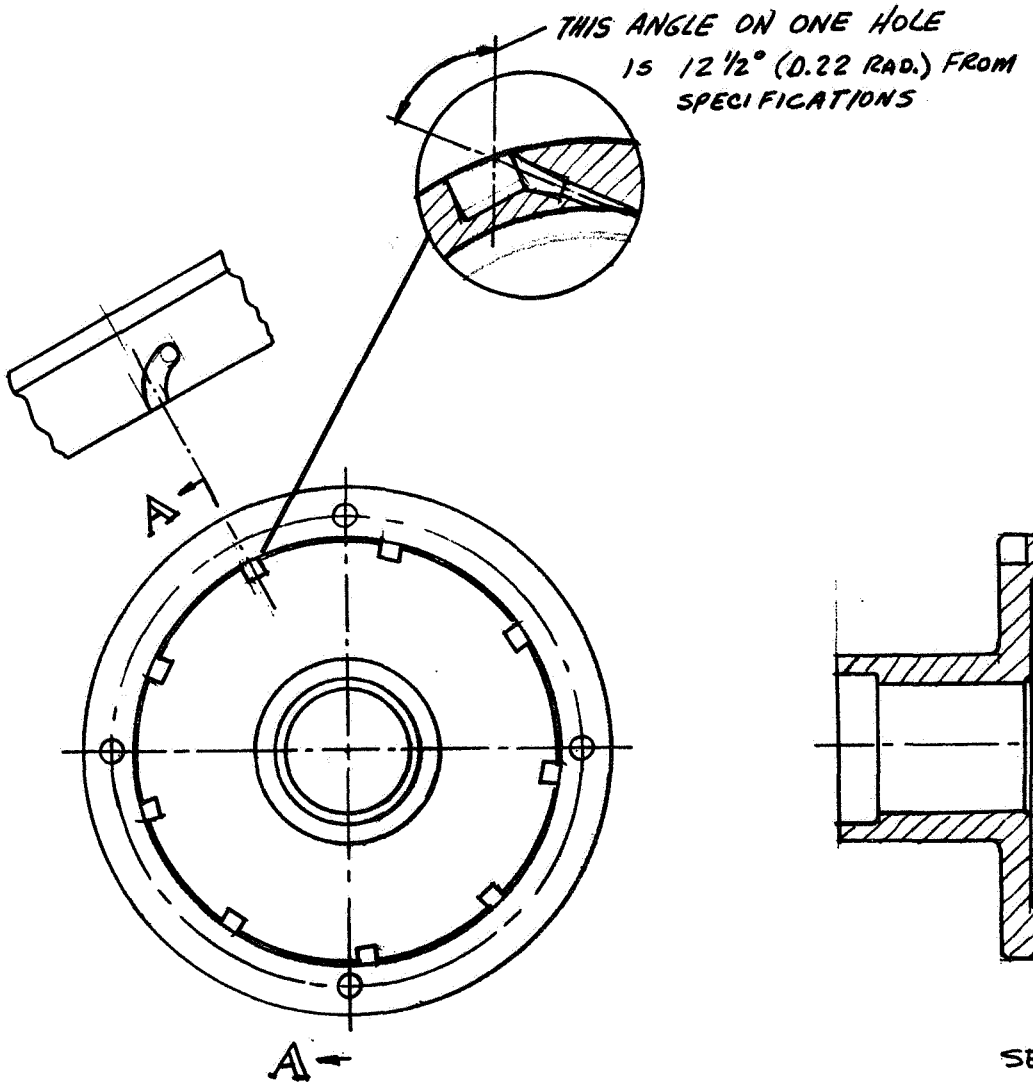


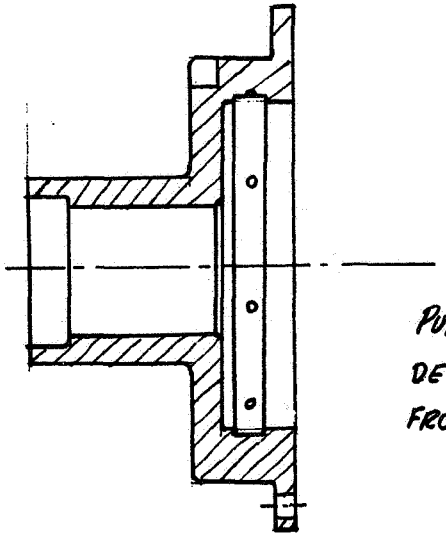

SECTION A-A

FIG. 6
PUMP DIFFUSER SHOWING
DEVIATION OF ONE HOLE
FROM SPECIFICATIONS

E-5338

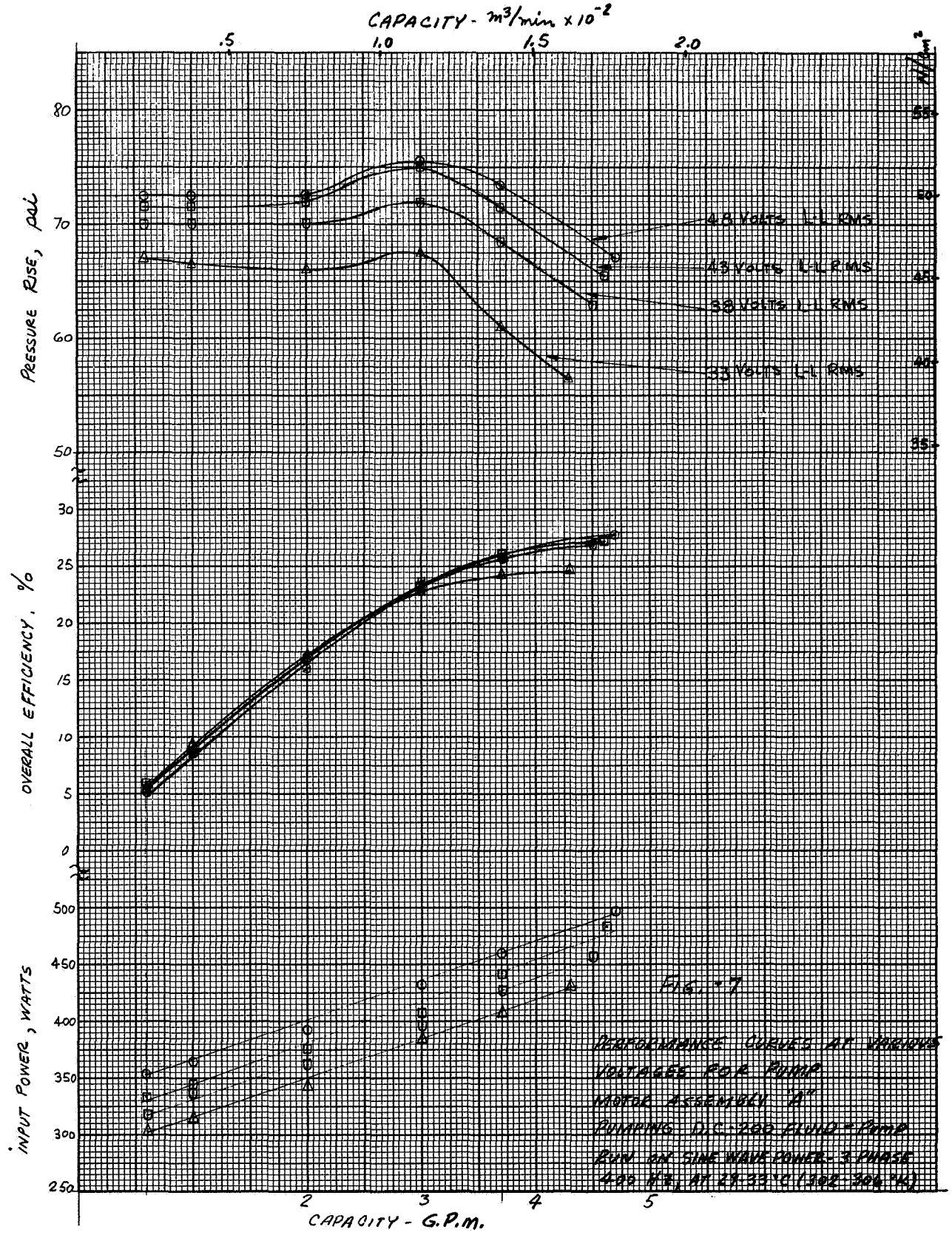


FIG. 7

PERFORMANCE CURVES AT VARIOUS VOLTAGES FOR PUMP MOTOR ASSEMBLY "A"

PUMPING D.C. 200 PSIG = PUMP RUN ON SINE WAVE POWER - 3 PHASE 400 Hz AT 27-33°C (302-304°K)

E-5538

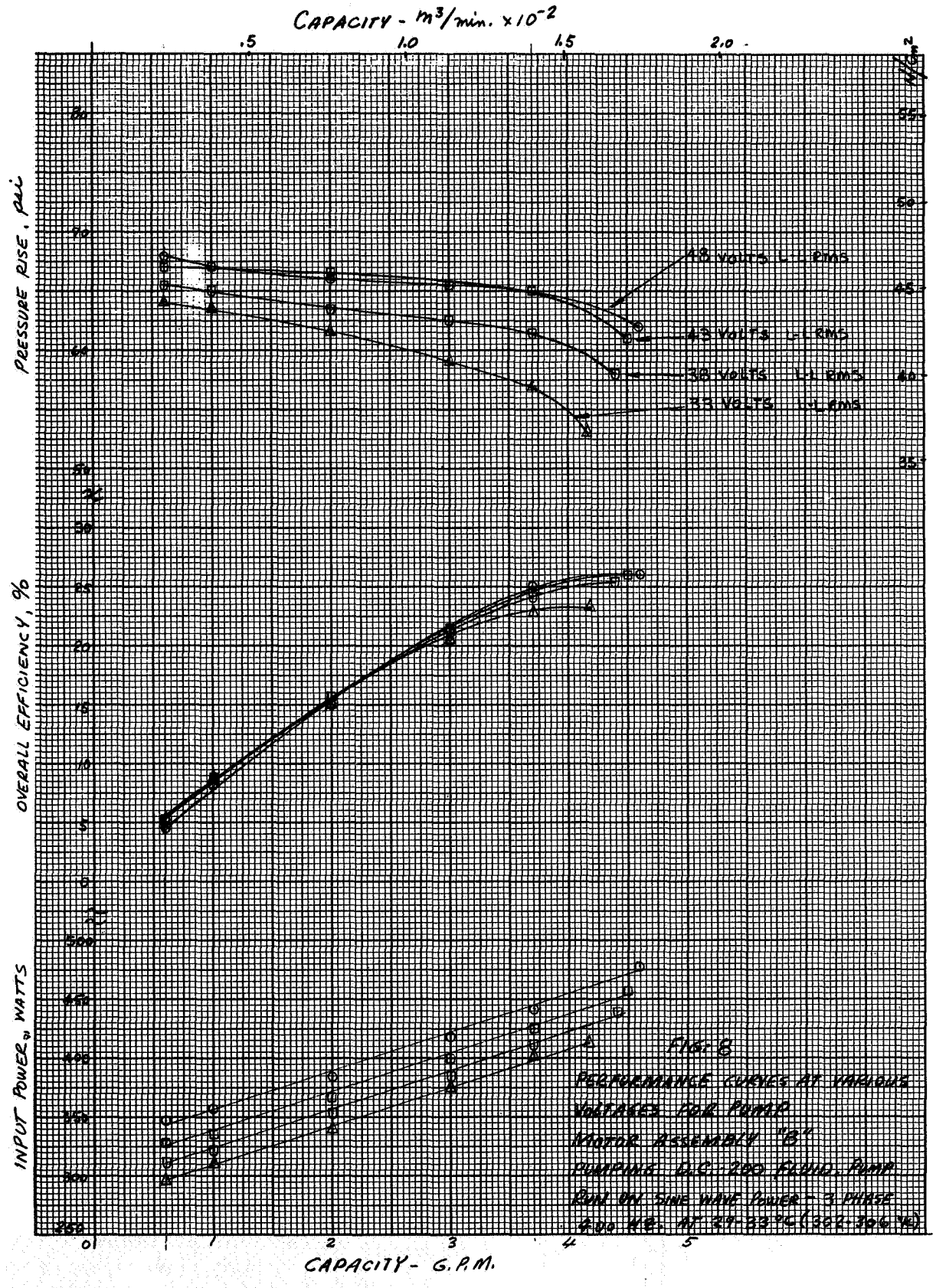


FIG. 6

PERFORMANCE CURVES AT VARIOUS VOLTAGES FOR PUMP MOTOR ASSEMBLY "B" PUMPING D.C. 200 FREON PUMP RUN ON SINE WAVE POWER - 3 PHASE 400 ~ AT 29.33°C (302.76 °K)

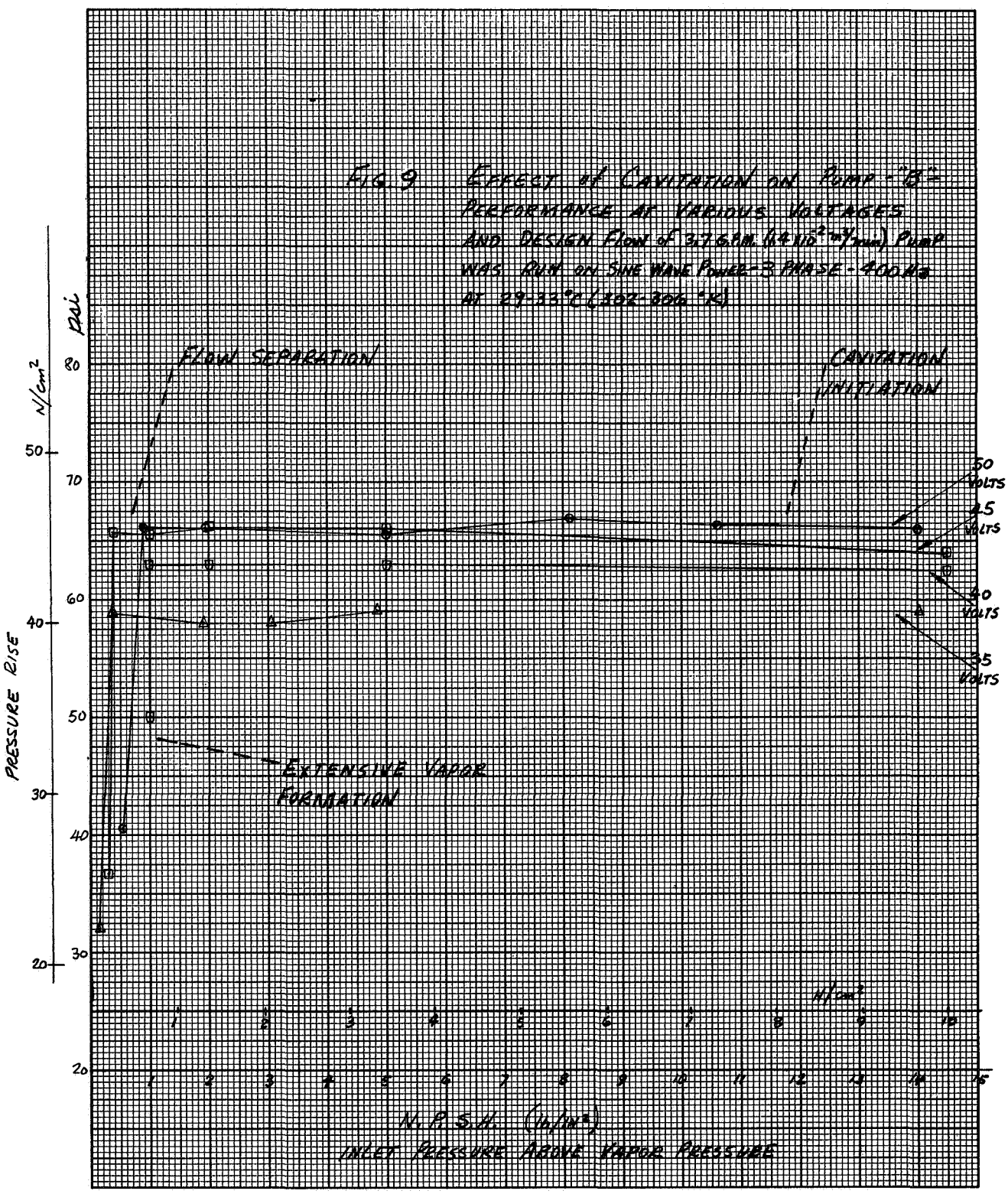


FIG. 9 EFFECT OF CAVITATION ON PUMP "B" PERFORMANCE AT VARIOUS VOLTAGES AND DESIGN FLOW OF 3.76 l/m. ($4 \times 10^{-2}$ m³/min) PUMP WAS RUN ON SINE WAVE POWER - 3 PHASE - 400 Hz AT 29-33°C (302-306 °K)

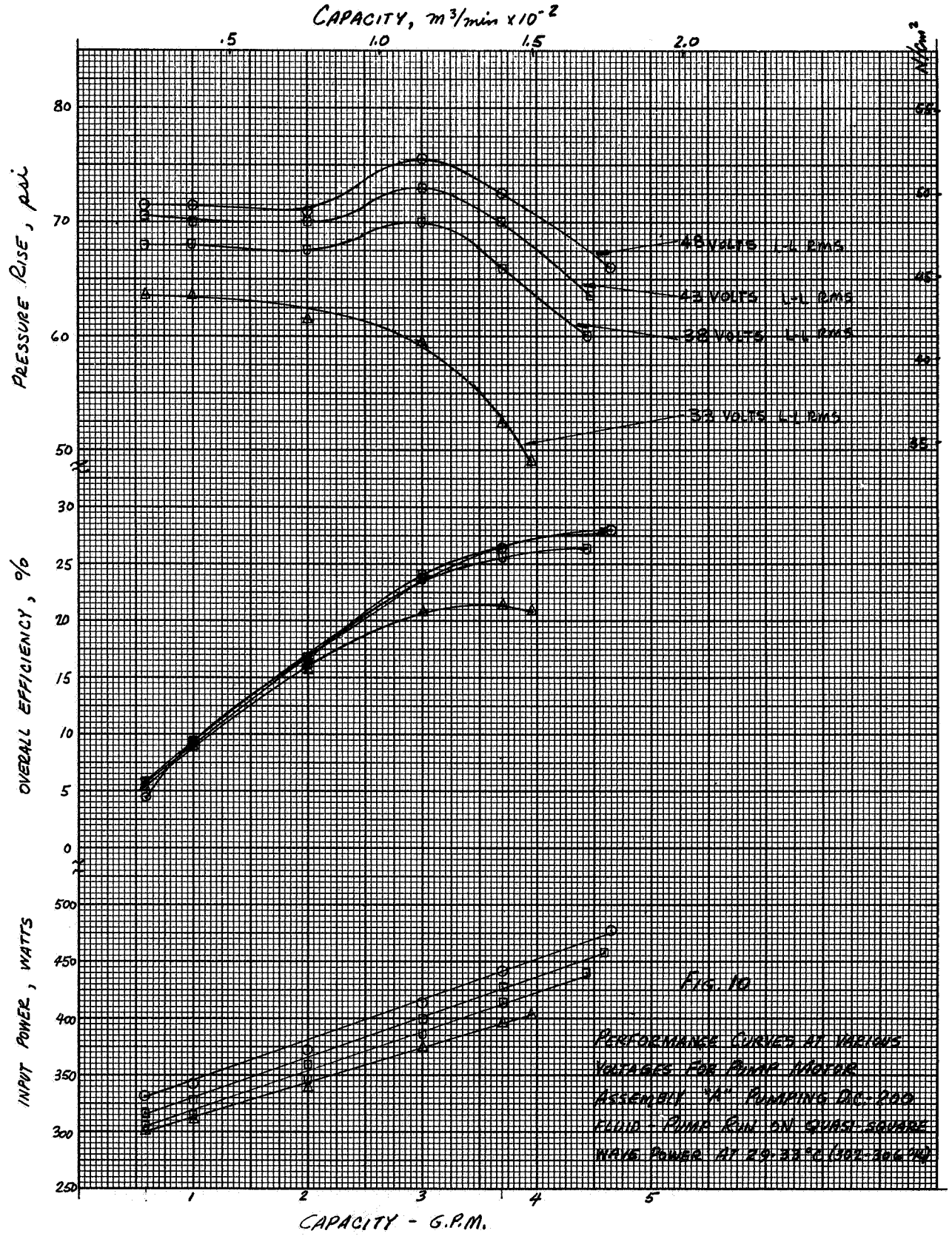


FIG. 10

PERFORMANCE CURVES AT VARIOUS VOLTAGES FOR PUMP MOTOR ASSEMBLY "A" PUMPING DC-200 FLUID. PUMP RUN ON SQUARE WAVE POWER AT 29-33°C (80°F-90°F)

E-5338

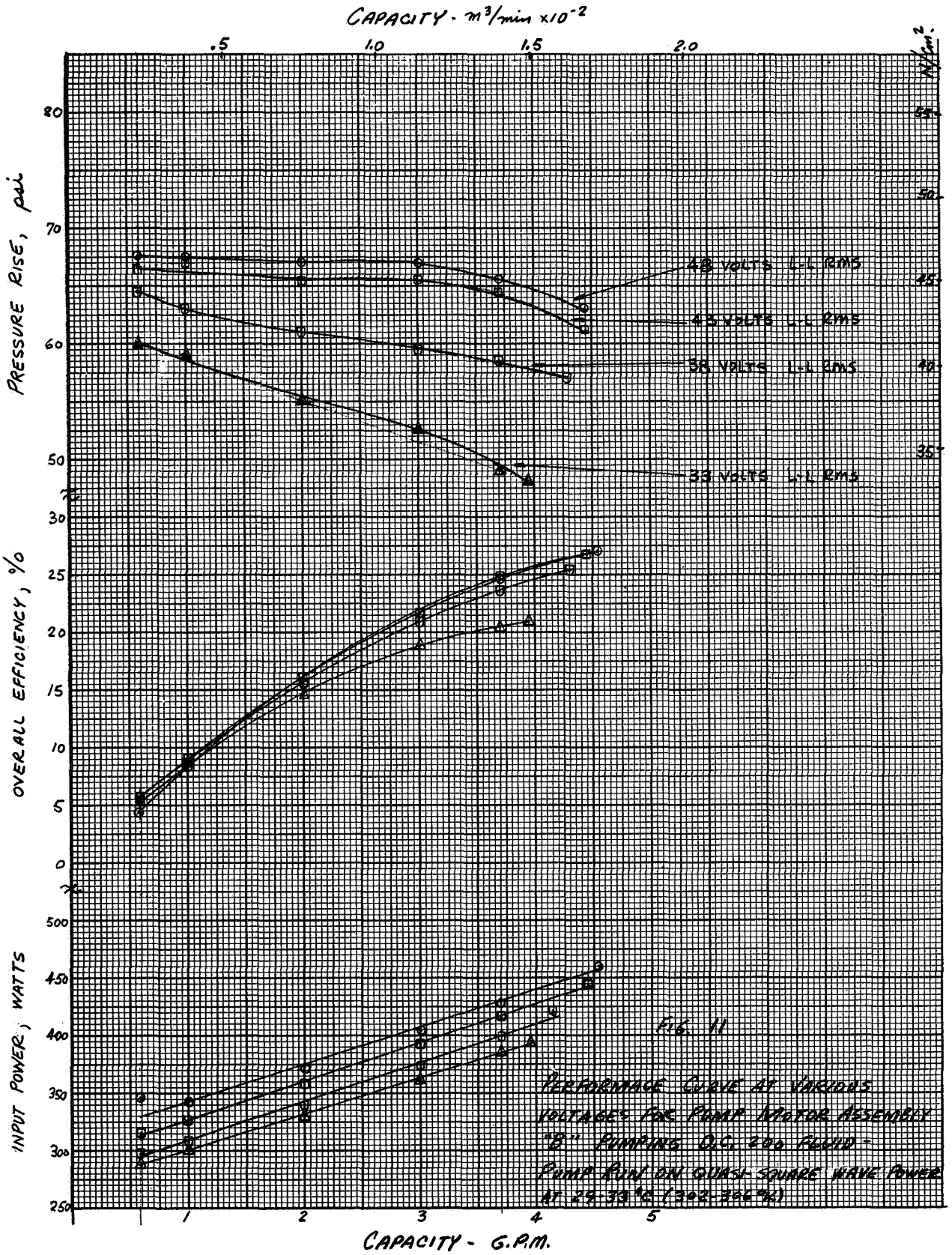


FIG. 11

PERFORMANCE CURVE AT VARIOUS VOLTAGES FOR PUMP MOTOR ASSEMBLY "B" PUMPING D.C. 200 FLUID - PUMP RUN ON QUASI-SQUARE WAVE POWER AT 29-33°C (302-306°K)

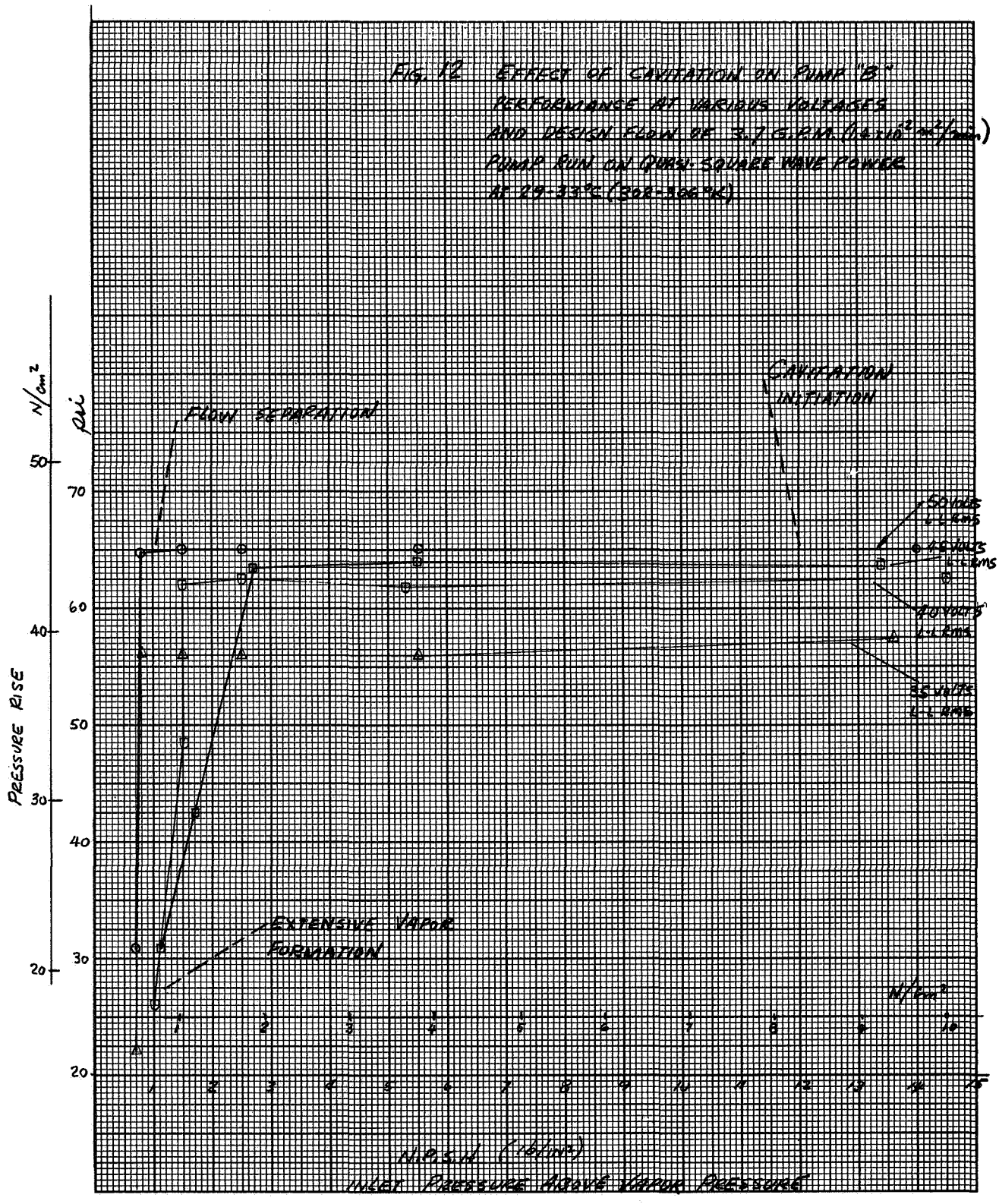


Fig. 12 Effect of Cavitation on Pump "B" Performance at Various Voltages and Design Flow of 3.7 G.P.M. ($0.4 \times 10^{-2}$ m³/sec.) Pump Run on Pure Square Wave Power at 29-33°C. (302-306°K).

E-5338

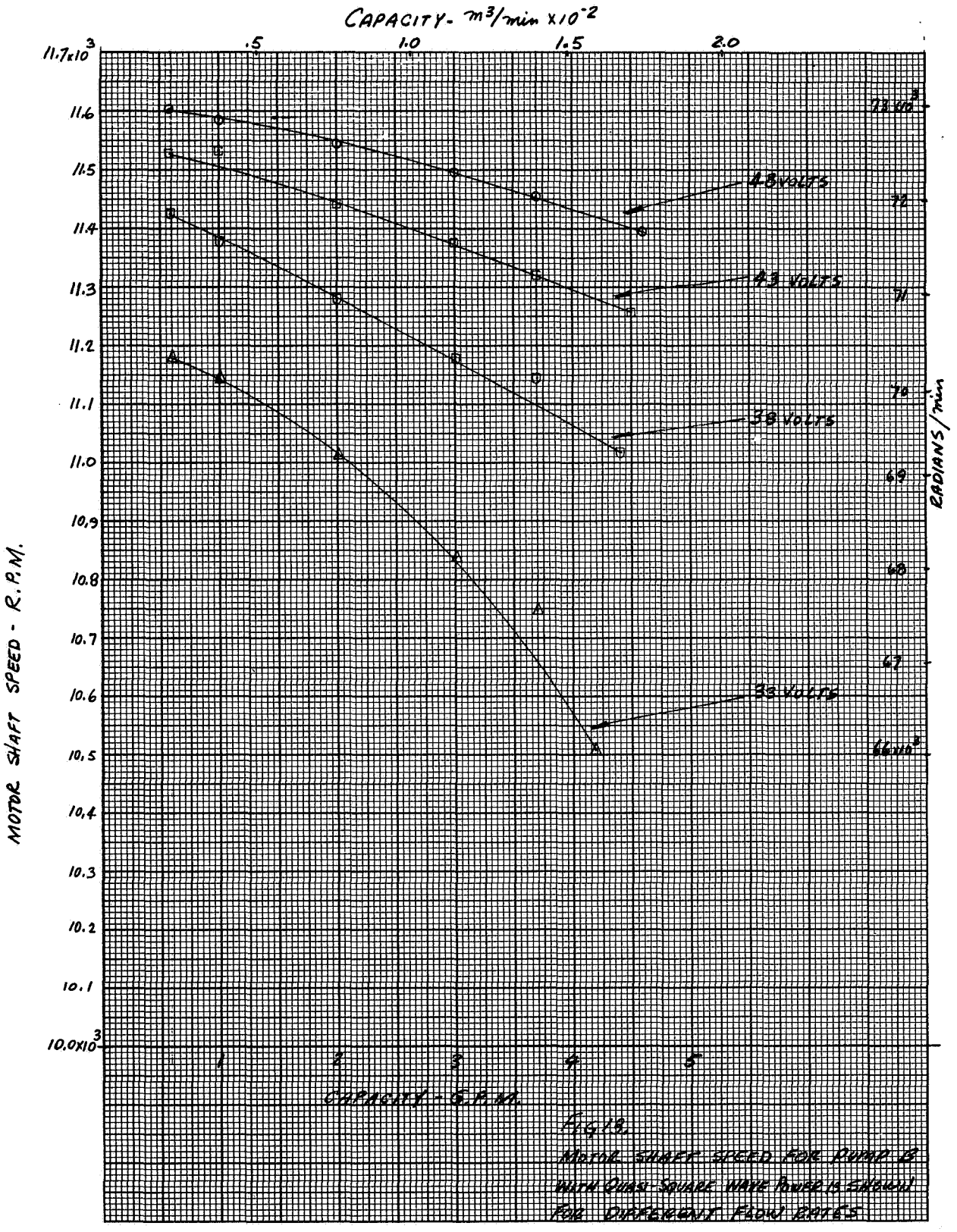


FIG 18.
MOTOR SHAFT SPEED FOR PUMP B WITH QUASI SQUARE WAVE POWER IS SHOWN FOR DIFFERENT FLOW RATES